DEVELOPMENT OF AN ADAPTIVE MULTIVARIABLE CONTROLLER FOR A REFRIGERATION SYSTEM USING TRANSFER FUNCTIONS GENERATED BY A WHITE BOX MATHEMATICAL MODEL

Maia, Antônio Augusto Torres
Fundação Universidade de Itaúna, Faculdade de Engenharia
Rodovia MG 431 - Km 45 – Campus Verde, 35680-142, Itaúna – Minas Gerais – Brasil.
aamaia@uit.br

Machado, Luiz
Universidade Federal de Minas Gerais, Departamento de Engenharia Mecânica
Av. Antônio Carlos, 6627, Pampulha, 31270-901, Belo Horizonte – Minas Gerais – Brasil.
luizm@demec.ufmg.br

Koury, Ricardo Nicolau Nassar
Universidade Federal de Minas Gerais, Departamento de Engenharia Mecânica
Av. Antônio Carlos, 6627, Pampulha, 31270-901, Belo Horizonte – Minas Gerais – Brasil.
koury@demec.ufmg.br

Abstract. *The interest for vapor compression refrigeration systems has increased considerably in the last decades. The optimization of these systems intending to improve its energetic efficiency has become one of the main goals in this field. An artifice that has been used is the refrigeration capacity control through the continuous adjustment of the compressor speed and the opening of the expansion valve according to the refrigeration demand. The algorithm that adjusts these variables requires information about the refrigeration system dynamic behavior to be developed. This information is generally obtained from experimental data, what is not always available. An alternative consists in using a mathematical model based on governing physical laws to generate these data through computer simulations. In this work it is intended to develop a mathematical model of a concentric tubes evaporator to generate the information needed to project an adaptive multivariable controller. The mathematical model, before being used in the controller development, was validated with experimental data. The results obtained showed that the proposed model can be used to describe the refrigeration machine dynamics and this information can be used to develop controllers.*

Keywords*: Refrigeration system, Mathematical model, Multivariable controller.*

1. Introduction

Refrigeration systems are great energy consumers and its operation is still considered inefficient. The capacity control method employed in most of these systems consists in a thermostat used to turn on and off the compressor in order to maintain the temperature between the desired levels. However, some researchers verified that this way of capacity control is responsible for efficiency losses as a result of the start up and shut down transients (Murphy et al., 1986; O'Neal et al., 1991; Radermacher and Kim, 1996; Pedersen et al., 1999). In this process, during the compressor off-cycle, refrigerant migrates from the condenser and the liquid line to the evaporator until the system pressure equalizes. This phenomenon increases evaporator temperature and became necessary a refrigerant redistribution during the on-cycle, what reduces the system efficiency (Coulter et al., 1997).

A more efficient capacity control method that has been utilized consists in adjusting continuously the compressor speed and the expansion valve opening regarding to the system thermal load (Tassou et al., 1998; Pedersen et al., 1999). The control algorithm responsible for defining the magnitude of these adjustments requires the knowledge of the refrigeration system dynamic model to be developed. This model is generally obtained from experimental data (black box model), what is not always available. Alternatively, a mathematical model based on governing physical laws (white box model) can be used to generate these data through computer simulations.

In this work it is intended to develop a mathematical model of a concentric tubes evaporator to generate the information needed to project an adaptive multivariable controller.

2. Mathematical model

The mathematical model developed in this work consists on the model of two components treated separately. In addition to the evaporator model it is also necessary the compressor model to estimate the mass flow rate at the outlet of this component. The mass flow rate estimated by both, the compressor and the evaporator model, are needed to be compared with each other at every time instant and used as one of the convergence criteria.

2.1. Compressor model

Some alternative type compressor models found in the literature are very complex, considering time and space discretization**.** This strategy generally permits a more accurate estimative of the pressure drop in the valves, the mass flow rate and the heat transfer coefficients. The compressor model developed in this work is very simple. On its implementation it was not considered: (1) Pressure drop in the valves; (2) Mass flow rate variation at the inlet and outlet; (3) The compressor thermal inertia. Along with these considerations it is assumed that: (4) The compression process is adiabatic.

In the compressor model, the input variables are the evaporation pressure (P_{f2}), the condensation pressure (P_{f3}) and the superheating degree (ΔT_s). The output variable is the mass flow rate at the outlet of the compressor ($\dot{m}_{f3}$). The mass flow rate estimative was done using the following expression:

$$\dot{m}_{f3} = N \cdot V \cdot \rho_{f2} \cdot \eta_v \tag{1}$$

where $\dot{m}_{f3}$, N, V, ρ_{f2} and η_v are respectively the mass flow rate, the rotational speed, the piston displacement volume, the specific mass at the compressor inlet and the volumetric efficiency. The volumetric efficiency can be estimated by the following equation:

$$\eta_v = 1 + c - c \cdot \left(\frac{P_{f3}}{P_{f2}} \right)^{\frac{1}{n}} \tag{2}$$

where c is the clearance ratio determined experimentally, P_{f3} and P_{f2} represent the condensing and evaporating refrigerant pressures. Once the compression process was considered adiabatic, n represents the quotient between the constant pressure and constant volume specific heats.

2.2. Evaporator model

In order to develop the evaporator model, the following simplifications were considered: (1) The refrigerant liquid and vapor phases are in thermodynamic equilibrium; (2) The axial heat transfer was neglected; (3) The evaporator has a perfect thermal insulation; (4) The physical properties related with refrigerant, secondary fluid and pipe wall were considered uniform in the evaporator cross section; (5) The refrigerant and secondary fluid potential energy was not taken into account.

In the evaporator model, the input variables are the refrigerant mass inside the evaporator (M), the mass flow rate ($\dot{m}_{f1}$) and the refrigerant enthalpy (h_{f1}) at the inlet of the evaporator, the secondary fluid mass flow rate ($\dot{m}_a$), the secondary fluid temperature (t_{a1}) at the inlet of the evaporator. The output variables are the refrigerant temperature at the inlet and outlet of the evaporator, the secondary fluid temperature at the outlet of the evaporator and various spatial patterns like pressure, enthalpy, temperature, etc.. The evaporator model was established by dividing this component into a number of control volumes and applying the principles of energy conservation (refrigerant, secondary fluid and pipes wall), as well as mass and momentum conservation (refrigerant). This procedure generates the following set of differential equations:

Refrigerant fluid (energy, mass and momentum conservation):

$$A_f \cdot \frac{\partial}{\partial t}\left[\rho_f \cdot (h_f - P_f \cdot v_f)\right] = -A_f \cdot \frac{\partial}{\partial z}(G_f \cdot h_f) + \alpha_f \cdot p_f \cdot (T_p - T_f) \tag{3}$$

$$\frac{\partial \rho_f}{\partial t} + \frac{\partial G_f}{\partial z} = 0 \tag{4}$$

$$\frac{\partial}{\partial z}\left\{P_f + G_f^2 \cdot \left[\frac{x^2 \cdot v_v}{\alpha} + \frac{(1-x)^2 \cdot v_l}{1-\alpha}\right]\right\} = -\frac{\partial G_f}{\partial t} - \left(\frac{dP}{dz}\right)_F - g \cdot \rho_f \cdot sin(\theta) \tag{5}$$

Secondary fluid (energy conservation):

$$\rho_a \cdot A_a \cdot c_{pa} \cdot \frac{\partial T_a}{\partial t} = -G_a \cdot A_a \cdot c_{pa} \cdot \frac{\partial T_a}{\partial z} - \alpha_a \cdot p_a \cdot (T_a - T_p) \tag{6}$$

$$\rho_p \cdot A_p \cdot c_{pp} \cdot \frac{\partial T_p}{\partial t} = \alpha_a \cdot p_a \cdot (T_a - T_p) - \alpha_f \cdot n \cdot p_f \cdot (T_p - T_f) \tag{7}$$

The subscripts f, p, a, l and v are related with refrigerant fluid, tube wall, secondary fluid, liquid and vapor phases, respectively. The variables A, G, h, T, P, p, x, ν, g, ρ, n and θ are the cross section area, the mass flux, the enthalpy, the temperature, the pressure, the wet perimeter, the vapor quality, the specific volume, the gravity acceleration, the specific mass, the number of tubes and the pipe inclination. The variable α when indexed represents the heat transfer coefficient and when it is not indexed it represents the void fraction. The mass flux can be estimated by the quotient between the mass flow rate and the cross section passage area. The refrigerant specific mass was computed using the following equation, where ρ_l and ρ_v are the liquid and vapor specific mass.

$$\rho = \rho_l + \alpha \cdot (\rho_v - \rho_l) \tag{8}$$

The correlations utilized in this work to estimate the heat transfer coefficient, the void fraction, and the pressure drop due the friction were obtained from the technical literature. To estimate the evaporation heat transfer coefficient, at first the evaporator was divided in three regions: evaporating region, liquid deficient region and superheating region. The quality and the critical quality ($x_{critical}$) were used as parameters to determine the start point and the end point of each region. The critical quality can be estimated through the correlation proposed by Sthapak (Maia, 2005):

$$x_{critical} = 7{,}943 \cdot \left[Re_v \cdot \left(2{,}03 \cdot 10^4 \cdot Re_v^{-0{,}8} \cdot (T_p - T_{sat}) - 1 \right) \right]^{-0{,}161} \tag{9}$$

where Re, T_p and T_{sat} are the Reynolds number, the wall tube temperature and the saturation temperature. Once defined the critical quality, the evaporating region was supposed to be settled while $x < x_{crittical.}$; the liquid deficient region was assumed to occur from $x = x_{critical}$ to $x = 1$ and the superheating region occurs when $x > 1$. For the evaporating region, the evaporation heat transfer coefficient (α_{eb}) was estimated using the correlation proposed by Dengler and Addoms (Maia, 2005). For the liquid deficient region (α_{def}), the heat transfer coefficient was estimated using a third order polynomial as presented bellow.

$$\alpha_{def} = a_0 + a_1 \cdot x + a_2 \cdot x^2 + a_3 \cdot x^3 \tag{10}$$

where x represents the quality. For the superheating region, the heat transfer coefficient (α_v) was estimated using the correlation proposed by Dittus-Boelter (Maia, 2005).To determine the coefficients (a_i) presented in the Eq. (10) it is needed four mathematical relations. These relations are:

$$\alpha_{def}(1) = \alpha_v(1) = a_0 + a_1 + a_2 + a_3 \tag{11}$$

$$\alpha_{def}(x_{critical}) = \alpha_{eb}(x_{critical}) = a_0 + a_1 \cdot x_{critical} + a_2 \cdot x_{critical}^2 + a_3 \cdot x_{critical}^3 \tag{12}$$

$$\left[\frac{\partial \alpha_{def}}{\partial x} \right]_{x=1} = \left[\frac{\partial \alpha_{def}}{\partial z} \cdot \frac{\partial z}{\partial x} \right]_{x=1} = a_1 + 2 \cdot a_2 + 3 \cdot a_3 = 0 \tag{13}$$

$$\left[\frac{\partial \alpha_{def}}{\partial x} \right]_{x=x_{critical}} = \left[\frac{\partial \alpha_{eb}}{\partial x} \right]_{x=x_{critical}} = \left[\frac{\partial \alpha_{eb}}{\partial z} \cdot \frac{\partial z}{\partial x} \right]_{x=x_{critical}} = a_1 + 2 \cdot a_2 \cdot x_{critical} + 3 \cdot a_3 \cdot x_{critical}^2 \tag{14}$$

In the Eq. (13) and (14), the variable z represents the position axis.

The void fraction was estimated using the correlation proposed by Hughmark. The pressure drop along the tubes for the two phase flow was compute by the Lockhart-Martinelli correlation and, for the single phase flow, it was used the correlation proposed by Fanning. Details about all correlations employed in this work can be found in Maia (2005).

The simultaneous solution of the Eq. (3) to (7) is very complicated due the fact that the refrigerant flow and the water flow are in opposite directions. To overcome this problem the Eq. (3) to (5) were solved separately using the fourth order Runge-Kutta method, along the z axis. The solution of the Eq. (6) and (7) was performed using the finite difference implicit method.

The proposed model was validated with experimental data in transient and steady state operating modes. The good agreement observed during this process showed that the proposed mathematical model and the numerical methodology utilized were effective in solving the problem. Details about the whole validation process can be found in Maia (2005).

3. Theoretical evaporator characterization

In order to develop an automatic controller, the proposed model was utilized in the dynamic characterization of the evaporator of the DEMEC-UFMG refrigeration machine. All data obtained in this process was employed to establish a dynamic relation between the input and the output variables. The system inputs are the expansion valve opening, which defines the mass flow rate ($\dot{m}_{f1}$), and the compressor speed, which defines the volumetric flow rate ($\dot{V}_{f2}$). The system outputs are the super heating (ΔT_s) and the refrigeration capacity ($\dot{Q}$). It was performed 8 simulations, covering the compressor speed of 650 rpm and 750 rpm and the evaporating temperature of -5°C, 0°C, 5°C and 10°C. At each operating point the system response to a step perturbation in the mass flow rate and volumetric flow rate was evaluated.

In the Fig. (1) is presented the theoretical response of the super heating and the refrigeration capacity to a step perturbation in the refrigerant mass flow rate. The simulation shown was performed utilizing an evaporation temperature of 0°C and a compressor speed of 750 rpm. Analyzing the figure it can be seen that the response of the refrigeration capacity is characterized by an initial variation in opposite direction of the final value (inverse response). The slight initial augment is because of the reduction of the evaporating temperature just before the perturbation launch, what reduces the water temperature at the outlet of the evaporator in an initial instant. After, the refrigeration capacity decreases as a consequence of the refrigerant mass reduction inside the evaporator. The super heating behavior is because of the refrigerant mass reduction inside the evaporator and its slow evolution is related with the thermal inertia of the evaporator.

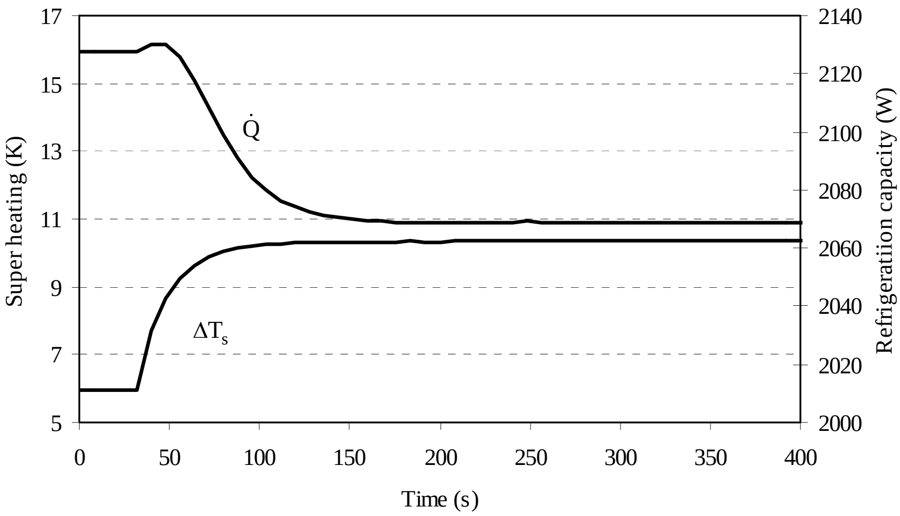

Figure 1 – Theoretical super heating and refrigeration capacity response to a step perturbation in the mass flow rate at the inlet of the evaporator (T_{eb}=0°C and N=750 rpm).

The super heating response was represented by a first order transfer function as presented below:

$$G_{11}(s) = \frac{\Delta T_s(s)}{\dot{m}_{f1}(s)} = -K_{11} \frac{1}{T_{11}\, s + 1} \quad (15)$$

where K, T and s are the static gain, the time constant and the Laplace variable. The static gain can be calculated by the ratio between the output variable variation and the input variable variation. The time constant represents the time instant that the super heating reaches 63% of the total variation. To represent the refrigeration capacity response, it was utilized a second order transfer function, as presented below:

$$G_{21}(s) = \frac{\dot{Q}(s)}{\dot{m}_{f1}(s)} = K_{21} \frac{(T_{21}\, s + 1)}{(T_{21}^{'}\, s + 1)(T_{21}^{''}\, s + 1)} \quad (16)$$

Once the simulations were performed for each operating point, it was possible to establish a mathematical relation for the time constant and static gain regarding to the compressor speed and the evaporation temperature. These relations are presented bellow:

$$K_{11} = 49.9776–0,1724*T_{eb}–2.6693*N+0.0094*T_{eb}*N \quad (17)$$

$$T_{11}=430.9446–1.4637*T_{eb}–9.8318*N+0.06867*T_{eb}*N \quad (18)$$

$$K_{21}=-199.2373+0.8267*T_{eb}+176.8967*N-1.1839*T_{eb}*N+0.002*T_{eb}^{2}*N \quad (19)$$

$$T_{21}'=353.7495-1.1785*T_{eb}-11.8836*N+0.0394*T_{eb}*N \quad (20)$$

$T_{21}''=333.2206-1.0206*T_{eb}-13.0019*N+0.038*T_{eb}*N$ (21)

$T_{21}=-168.9567+0.5063*T_{eb}+16.0406*N-0.0534*T_{eb}*N$ (22)

Where N is the compressor speed given in revolutions per second and T_{eb} is the evaporating temperature given in Kelvin.

Figure (2) presents the theoretical response of the super heating and the refrigeration capacity to a step perturbation in the refrigerant volumetric flow rate. The simulation shown was performed utilizing an evaporation temperature of 0°C and a compressor speed of 750 rpm. In this figure it can be noticed that the refrigeration capacity is not substantially influenced by the step perturbation. The small increase observed at first is due to the augment in the compressor speed that promotes an enlargement in the volumetric flow rate at the outlet of the evaporator. Following, the refrigeration capacity diminishes close to the initial value. This occurrence is due to the increase of the super heating at the outlet of the evaporator, which promotes a reduction in the refrigerant specific mass and a resulting decrease of the refrigerant mass flow rate at the outlet of the evaporator. The final value of the refrigeration capacity is slightly higher (about 2%) than the initial value because when the super heating increases, the enthalpy at the outlet of the evaporator also increases.

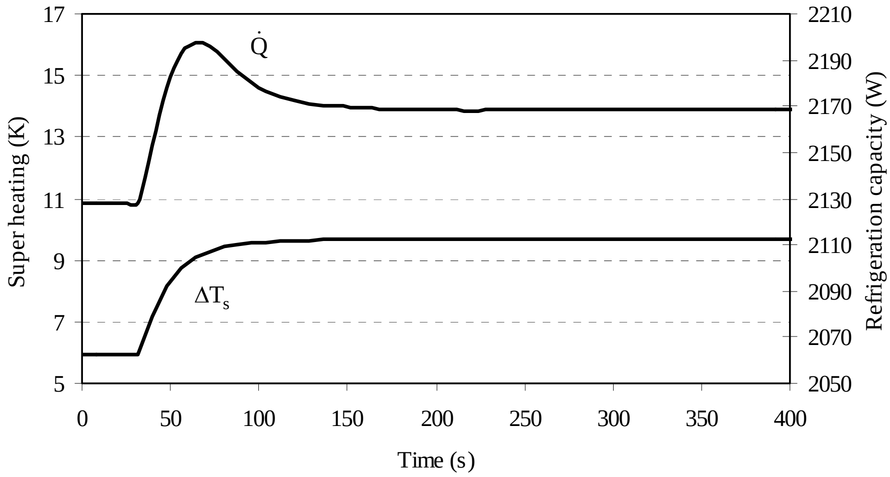

Figure 2 – Theoretical super heating and refrigeration capacity response to a step perturbation in the volumetric flow rate at the outlet of the evaporator (T_{eb}=0ºC and N=750 rpm).

Although the super heating response in the Fig.(2) is a typically first order response, it was obtained a better curve fitting when using a second order transfer function, as presented bellow:

$$G_{12}(s)=\frac{\Delta T_s(s)}{\dot{V}_{f2}(s)}=K_{12}\,\frac{(T_{12}s+1)}{(T_{12}'s+1)(T_{12}''s+1)} \quad (23)$$

To represent the refrigeration capacity response, it was utilized a second order transfer function, as presented below:

$$G_{22}(s)=\frac{\dot{Q}(s)}{\dot{V}_{f2}(s)}=K_{22}\,\frac{(T_{22}s+1)}{(T_{22}'s+1)(T_{22}''s+1)} \quad (24)$$

The mathematical relations for the time constant and static gain regarding to the compressor speed and the evaporation temperature are presented below:

$K_{12}=487.4332-1.6231*T_{eb}-27.4981*N+0.091*T_{eb}*N$ (25)

$T_{12}'=1286.4307-4.4911*T_{eb}-80.7884*N+0.2834*T_{eb}*N$ (26)

$T_{12}''=180.3952-0.6227*T_{eb}-0.7847*N+0.0032*T_{eb}*N$ (27)

$T_{12}=188.4392-0.6382*T_{eb}-6.096*N+0.0197*T_{eb}*N$ (28)

$K_{22}=-401.1533+2.2716*T_{eb}-196.4686*N+0.7071*T_{eb}*N$ (29)

$$T_{22}'=588.9251-1.8951*T_{eb}-30.8759*N+0.09996*T_{eb}*N \quad (30)$$

$$T_{22}''=696.3566-2.3912*T_{eb}-42.2744*N+0.1477*T_{eb}*N \quad (31)$$

$$T_{22}=1755.4812-5.5721*T_{eb}-47.1929*N+0.1305*T_{eb}*N \quad (32)$$

4. Controller and pre-compensator project

The dynamics of the refrigeration system in study can be represented by the following transfer function matrix:

$$\begin{bmatrix} \Delta T_s(s) \\ \dot{Q}(s) \end{bmatrix} = \begin{bmatrix} G_{11}(s) & G_{12}(s) \\ G_{21}(s) & G_{22}(s) \end{bmatrix} \begin{bmatrix} \dot{m}_{f1}(s) \\ \dot{V}_{f2}(s) \end{bmatrix} \quad (33)$$

where G_{ij} is the transfer function that relates the i output with the j input. Each of these transfer functions was obtained in the precedent section through simulations. The Eq. (33) represents a multivariable system with cross coupling (each of the outputs is function of both inputs). In this case, the controller project can be divided in two steps. The first step consists in developing a mechanism to minimize the cross coupling, and the second step consists in developing the controller. One way to minimize the cross coupling is using a pre-compensator to become the original system diagonal dominate in some frequency range. In the case studied, to guarantee a good performance in steady-state, the system must be decoupled in low frequencies (0 rad/s). Rewriting the Eq. (33) as:

$$[Y(s)] = [G(s)]\,[U(s)] \quad (34)$$

The diagonal dominance can be achieved applying the following pre-compensator (Skogestad et al., 2003):

$$[W(0)]=[G(0)]^{-1} \quad (35)$$

In many systems it is possible to establish a relation between the process dynamics and the operation conditions. With this relation it is possible to reduce the effects of the operating point changes defining certain controller parameters as function of these operation conditions. This strategy can be applied to adjust the pre-compensator parameters. Solving the Eq. (35), the pre-compensator presents the following form:

$$[W(s)]=\begin{bmatrix} -K_{11} & K_{12} \\ K_{21} & K_{22} \end{bmatrix}^{-1} \quad (36)$$

where K_{ij} represents the static gain of the Eq.(15), (16), (23) and (24). Once it was established dynamic relations to express these variables regarding to compressor speed and evaporating temperature, these relations can be used to adjust the pre-compensator and reduce the effects of the operating point changes.

Since the system with the pre-compensator is diagonal dominate in low frequencies, a PI controller can be designed to minimize the steady-state error:

$$[C(s)]=\begin{bmatrix} K_{p1}+\dfrac{K_{i1}}{s} & 0 \\ 0 & K_{p2}+\dfrac{K_{i2}}{s} \end{bmatrix} \quad (37)$$

where K_p and K_i represent the proportional and integral gains. A diagonal controller can be determined associating the pre-compensator (Eq. (36)) and the PI controller (Eq.(37)):

$$[C_d(s)]=\frac{1}{-K_{11}\times K_{22}-K_{12}\times K_{21}}\times\begin{bmatrix} K_{22} & -K_{12} \\ -K_{21} & -K_{11} \end{bmatrix}\times\begin{bmatrix} C_{11}(s) & 0 \\ 0 & C_{22}(s) \end{bmatrix} \quad (38)$$

In the Fig. (3) is presented the block diagram for the closed loop system. The system has two feedbacks: The first one is the traditional feedback and the second is the adaptation feedback. This last is responsible for adjusting the pre-compensator parameters based on the operation conditions.

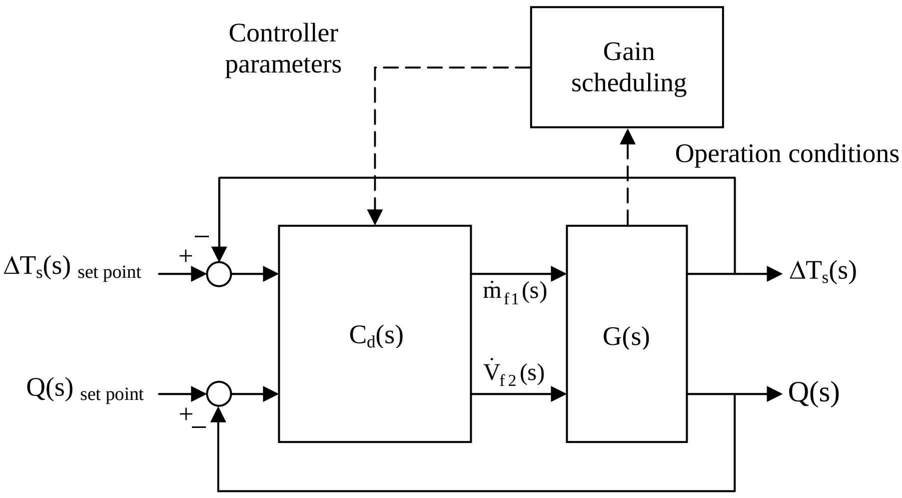

Figure 3 - Block diagram for the closed loop system

Finally, the closed loop transfer function has the form:

$$T(s) = G(s)\,W(s)\,C(s)\left[\,I + G(s)\,W(s)\,C(s)\,\right]^{-1} \tag{39}$$

To evaluate the controller performance simulations were performed using Matlab-Simulink. The PI controller gains utilized in these simulations were K_{p1}=0.2; K_{i1}=0.04 and K_{p2}=22.0; K_{i2}=1.5. In the Fig. (4), (5) and (6) is presented the super heating and the refrigeration capacity response to a step perturbation.

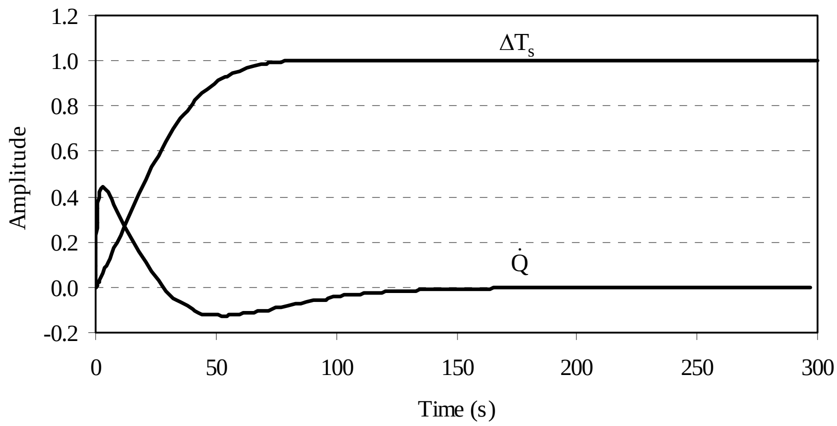

Figure 4 - Super heating and refrigeration capacity response to a step perturbation in the super heating ($\Delta T_{s\ set\ point}$=1 and $Q_{set\ point}$=0).

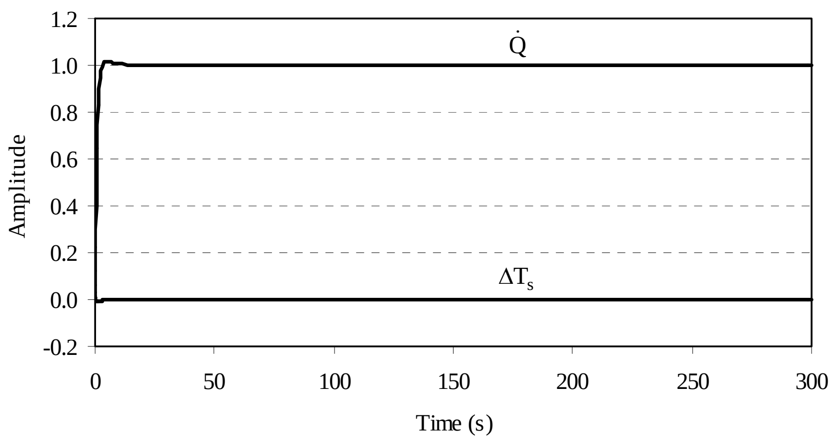

Figure 5 - Super heating and refrigeration capacity response to a step perturbation in the refrigeration capacity ($\Delta T_{s\ set\ point}$=0 and $Q_{set\ point}$=1).

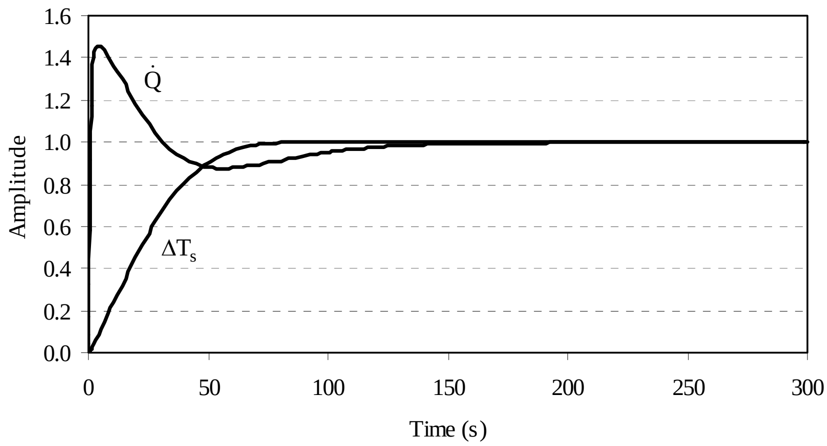

Figure 6 - Super heating and refrigeration capacity response to a step perturbation in the refrigeration capacity and super heating ($\Delta T_{s\ set\ point}$=1 and $Q_{set\ point}$=1).

In the Fig. (4), (5) and (6) it should be noticed that the controller was effective. The low frequencies decoupling became possible the independent control of the super heating and the refrigeration capacity. These results can be improved selecting other controller gains. All simulations were carried out for T_{eb}=10.7^{o}C and N=650 rpm. Other operating points were also evaluated and similar results were obtained.

5. Conclusions

In this work a white box mathematical model was developed and utilized in the dynamic characterization of a refrigeration machine. Employing the data obtained in this process, it was developed a multivariable controller for the system studied. The proposed controller was able to regulate the refrigeration capacity and the super heating in an independent way, demonstrating that the pre-compensator utilized was effective in minimizing the cross coupling. The relations established to describe the gain and time constant regarding to evaporating temperature and compressor speed were employed to adjust the pre-compensator parameters regarding to the operation point.

6. References

Coulter, William H. and Bullard, Clark W., 1997, "An experimental analysis of cycling losses in domestic refrigerator-freezers" ASHRAE Transactions, v. 103, part 1, pp587-596.

Maia, Antônio A. T., 2005, "Metodologia de desenvolvimento de um algoritmo para controle simultâneo da capacidade de refrigeração e do grau de superaquecimento de um sistema de refrigeração", Tese (Doutorado), Departamento de Engenharia Mecânica, Universidade Federal de Minas Gerais, Belo Horizonte, 160 pp.

Murphy, W. E. and Goldschmidt, V. W., 1986, "Cycling characteristics of a residential air conditioner-modeling of shutdown transients", ASHRAE Transactions, v. 92, part 1A, pp186-202.

O'Neal, D. L. and Katipamula, S., 1991, "Performance degradation during on-off cycling of single-speed air conditioners and heat pumps: Model development and analysis", ASHRAE Transactions, v. 97, part 2, pp316-323.

Pedersen, P. H., Poulsen, C. S. and Gundtoft, S., 1999, "Refrigerators and freezers with variable speed compressors" 20th International Congress of Refrigeration IIR/IIF, Sydney, p.1-7, paper code 153, preprints.

Radermacher, R. and Kim, K., 1996, "Domestic refrigerators: recent developments", International Journal of Refrigeration, v. 19, Nº 1, pp 61-69.

Skogestad, S. and Postlethwaite, I. 2003, "Multivariable Feedback Control – Analysis and Design", John Wiley & Sons.

Tassou, S. A. and Qureshi, T. Q., 1998, "Comparative performance evaluation of positive displacement compressors in variable speed refrigeration applications" International Journal of Refrigeration, v. 21, Nº 1, pp29-41.

7. Responsibility notice

The authors are the only responsible for the printed material included in this paper.